Journal of Cleaner Production 264 (2020) 121475

Contents lists available at ScienceDirect

Journal of Cleaner Production

journal homepage: www.elsevier.com/locate/jclepro

Economic pipe diameter of settling slurries

Christian F. Ihle [a, b, *]

[a] Department of Mining Engineering, Universidad de Chile. Beauchef 850, 8370448, Santiago, Chile
[b] Advanced Mining Technology Center, Universidad de Chile. Tupper, 2007, Santiago, Chile

ARTICLE INFO

Article history:
Received 8 March 2018
Received in revised form
28 March 2020
Accepted 30 March 2020
Available online 16 April 2020

Handling Editor: Jiri Jaromir Klemeš

Keywords:
Pipelines
Energy efficiency
Economic pipeline size
Embodied energy
Settling slurries
Mining industry

ABSTRACT

The notion of economic pipe size is extended to the case of settling slurries, which are commonly found in high tonnage, long distance pipelines of mineral ores. Water, energy and pipe infrastructure costs have been considered under the premise that the objective of this kind of infrastructure is to transport solids but not water. Unit costs for pipes have been expressed based on pipe weight or diameter. In the first case, both an assumption of a linear dependency of the pipe wall thickness with outside diameter and the special case of prescribed, outside diameter-independent pipe wall thickness, have been considered. On the other hand, a typical assumption of cost expressed as a potential function of the pipe diameter has been assumed to compare with the present model. A dimensionless formulation of the problem, including the requirement of turbulent flow transport above the deposit limit is proposed. Differently from previous analyses, made for homogeneous fluids, the present approach does not require a particular form of the friction factor. To this purpose it is shown, based on the general form of the dependency of the friction factor with the Reynolds number, that the friction factor that minimizes the operation and infrastructure cost is the maximum possible within the turbulent regime, *i.e.* that corresponding to the laminar-turbulent transition. Optimal conditions feature: (1) the solid concentration should be the largest possible provided safe transport is ensured, (2) the optimal pipe diameter is controlled either by costs and turbulent transition or by the deposit limit condition (not both of them simultaneously), where a dimensionless parameter has been derived to identify the relevant solution. Results with the present cost scheme have been extended to the case of homogeneous fluids.

1. Introduction

The notion of economic pipeline is not new when conveying water or homogeneous fluids. In this case, the economic pipeline diameter is commonly computed as that resulting of the sum of the steel, maintenance and energy costs. The first analysis of economic pipeline diameter for compressing or pumping has been made by Genereaux (1937), who considered a number of economic metrics including amortization, maintenance, a factor for fittings and erection that were taken into account as part of single-phase optimization. After a number of assumptions, including an explicit modeling of pressure losses *via* the Fanning friction factor (for turbulent flow) in terms of the Reynolds number and a set of unit costs, he proposed an economic diameter in the form G^a/ρ^b (in his work, $(a,b)=(0.448, 0.315)$), where G and ρ are the fluid throughput and density, respectively. The approach made for this was finding the minimum diameter by differentiation of the cost function. The economic parameters used in his work have been updated to 2008 by Durand et al. (2010). Contemporary to Genereaux (1937), Sarchet and Colburn (1940) extended his nomographs to laminar flow and obtained a slightly different result for turbulent flow, for diameters above and below 1inch. The addition of tax effects and return of investment in laminar and turbulent transport systems is discussed in Peters et al. (2002). In their results, they found that for a fluid tonnage on the order of $200 kg/s$, a difference of about one commercial diameter compared with the a simplified cost approach exists. In a smaller throughput case ($G=2kg/s$) they found a similar relative difference. An assumption common to the works referred herein is that for pipeline nominal diameters above $1in$, the annual cost for the installed piping system is proportional to D^n, where $n\approx1.5$ for carbon steel pipes and varies according to transported fluid, pressure rating of the pipe and market conditions (Darby, 2001; Genić et al., 2012; Genić and Jaćimović, 2018).

* Corresponding author. Department of Mining Engineering, Universidad de Chile. Beauchef 850, 8370448, Santiago, Chile.
E-mail address: cihle@ing.uchile.cl.

https://doi.org/10.1016/j.jclepro.2020.121475
0959-6526/

The problem of optimal pipe diameter in generalized fluids has been treated after the major development on the characterization of friction losses in this kind of system (Metzner and Reed, 1955; Dodge and Metzner, 1959). Garcia and Steffe (1986) proposed an explicit relationship for Herschel-Buckley fluids in laminar flow. In their derivation, they follow the same pipe diameter/cost scaling as in the Newtonian case. An iterative framework for the computation of optimal pipe size, including non-Newtonian fluids is discussed by Darby (2001).

Fine slurries may be conditionally understood as a special type of non-Newtonian fluid. When fully mixed and if transport is homogenous they are commonly treated as Bingham or Herschel-Buckley fluids (Bird et al., 1983; Ricks, 2002). However, depending on the characteristics of the solid phase, including concentration and particle size, they may segregate (Turian and Yuan, 1977), thus creating operational risks related to plugging, especially in long distance systems (Ihle, 2014b). In slurries, a solid phase is relevant due to its effect on energy consumption and greenhouse emissions (Ihle, 2014). Is it common that the fluid (liquid) phase is merely a vehicle required for the solid phase transport, which is often lost and thus constitutes a cost (Ihle et al., 2014), which can be considerable high given that commonly slurry transport systems span distances that can reach hundreds of kilometers to replace rail roads (Jacobs, 1991; Abulnaga, 2002). The required energy, on the other hand, is that resulting from transporting not just the solid phase, but also the water phase. When put together, water an energy configure an equivalent fluid whose transport conditions face the critical trade-off of energy and infrastructure requirements. The problem departs from that of designing water (or homogeneous fluid) lines in two critical aspects: (1) when transporting slurries, the relevant process variable for energy, and ultimately cost efficiency enhancement is throughput (solid phase transport), not water and (2) the mean flow velocity cannot be arbitrarily small, as particles tend to form solid deposits in the pipeline and thus cannot be transported. The second aspect is effectively a process restriction, while the first one implies the introduction of the concept of solids concentration in the choice of the infrastructure/process condition combination. A potentially third aspect to consider is the need to transport within a specific flow regime (either laminar or turbulent). In water pipelines, normally facilities are designed for turbulent flow because laminar flow would imply prohibitively high transport costs. In the case of slurry pipelines, the flow regime can be either laminar or turbulent, the former case corresponding to paste slurries behaving as 'stabilized', homogeneous fluid (Paterson, 2012) while the latter is associated to lower volume concentrations, and is commonly the preferred regime for long distance transport (Abulnaga, 2002; Ihle and Tamburrino, 2012).

Given that slurry pipelines commonly connect long distances, sub-optimal choices of their diameter may be related to strong additional costs. As an example, a 1-inch difference using a SCH80 pipe pressure rating (say, between 5 and 6 inches in diameter) in a 100 km-line would cost, considering a $15 USD/kg_{\mathrm{steel}}$ scenario a difference of about 17.4MUSD, whereas differences in the range 22in–24in imply more than 100MUSD difference. In engineering practice, the determination of the economic settling slurry pipe diameter is limited to the identification of the diameter associated to the limiting velocity for the formation of deposits, commonly referred to as the *deposit velocity*. Recently, this condition has been effectively identified as that which minimizes the energy and water costs given the pipe diameter (Ihle, 2016). However, the intuitive notion that the determination of the optimal diameter should be, in principle, dependent on the pipe infrastructure cost, suggests an extended formulation including such variable. In the present paper, the concept of optimal diameter for settling slurries is introduced, and a simple model is proposed to assess the most economic pipeline diameter based on the aspects referred above. To the best knowledge of the author, the only previous approach to this exact problem has been explored by Ihle et al. (2013) using a sequential quadratic programming optimization approach in a limited number of system throughputs and cost scenarios. Although a number of optimal scenarios could be identified therein, conditions were very particular, motivating the present extension.

The paper structure is as follows: in Section 2, the problem formulation is given, including the declaration of all the hypotheses in the analysis. In Section 3, the water, energy and pipe material cost equation is rendered dimensionless to proceed to the construction of the model. Section 4 presents derived expressions for economic pipe diameter. Dimensional results, useful for practical purposes, are given on equations 36–41. From the present analysis, a new equation for the case of a homogeneous fluid (without the presence of settling particles whatsoever) is proposed on equation (42). The corresponding notation for all expressions is described throughout the document and are summarized, including units, on page List of symbols. In the same section, the sensitivity of results is analyzed in light of the most important parameters of the model and additional aspects such as conciliation of results with operational pressure are discussed as well. The model is exemplified with published pipeline data and a number of cost scenarios in Section 4.6. Final remarks are given in Section 5.

2. Problem formulation

The problem is to estimate the lowest cost operational and pipeline diameter combination in industrial pipelines, given the throughput (solid phase transport rate) requirement, the pipeline topography and the operational life of the infrastructure. The formulation of the present problem implies that higher pipeline diameters reduce the energy consumption as velocities are lower, but increment the pipe cost. On the other hand, there is a cost related to water. Therefore, there is a trade-off between energy consumption, particle concentration and required throughput. There is a solid phase mass balance that acts an a restriction of the problem. Additionally, the fact that given a pipe diameter there is a critical mean flow velocity that marks a settling limit acts as a restriction for the potential solutions of the problem. While in a traditional optimization approach for optimal pipeline diameter it is straightforward to derive the minimum cost diameter via differentiating the cost function, equating to zero and solving for the diameter, in this case the referred constraints act as limiting factors that need to be accounted for.

2.1. Assumptions

The following assumptions hold in the present approach to the solution of the problem:

1. The operational throughput is a constant of the problem, and is defined by the transport service characteristics.
2. The life of operation of the project is known.
3. Given a throughput range, the rest of the components of the construction cost, including trench dimensions in buried systems, pumps and possibly dissipation stations are weakly dependent on the identification of the optimal pipeline diameter and thus can be omitted from the present analysis. This is equivalent to assume that such costs are piecewise constant in a reasonably wide range of throughputs.
4. Singular pressure losses due to elbows, valves, etc., are negligible when compared to frictional losses.
5. Maintenance costs to operate facilities are virtually constant both with pipeline diameter and solids concentration, and

thus are not amenable to be optimized in terms of these variables.

6. The pipeline route is fixed (or previously selected), and thus pipeline length and the corresponding earthworks (as discussed, *e.g.*, in Baeza et al., 2017) are not subject to optimization.
7. Unit costs for energy, water and (installed) pipeline per unit weight can be estimated and set constant in the problem.
8. The pipeline has a circular cross section and constant wall thickness throughout its length. Thus, some coefficients indicated herein (including factors of π) correspond to such geometry.
9. There is a pre-established relation between the pipeline thickness, the pipeline internal diameter (D) and the pipeline cost.
10. The flow of slurries is such that they are amenable to be transported as an homogeneous (or quasi-homogeneous) suspension. There is a deposit limit that can be described as a function of one or more characteristic parameters and its dependence on the particle concentration can be neglected. The mean flow velocity needs to exceed the minimum velocity to avoid deposit formation.
11. To complement the previous hypothesis, it is required that transport is in turbulent flow. Additionally, laminar-turbulent transition can be described through a single dimensionless parameter (a Reynolds number). This implies that near transition the flow is hydraulically smooth.
12. As the intent of hydraulic transport is to convey the solids rather than water, solid concentration will not be within the dilute range. The present problem is thus treated under the assumption that moderate to high solid concentrations are used for transport. Thus, the parameter that describes the deposit formation (named to herein as the Durand number) is assumed to be weakly dependent on the solids concentration. This is discussed in Section 3.
13. There is a maximum safe operational concentration beyond which transport is not allowed.
14. The pumping efficiency has a negligible dependence on the concentration, within the concentration range of interest for optimization, and therefore can be treated as a constant. This assumption is reasonable when positive displacement pumps are used, which is the case in the high pressure systems.
15. The system is not allowed to generate energy, as would occur in pipelines with a slope such that the energy consumption is exceeded by the potential-to-kinetic energy conversion. The justification of this assumption is that an energy generation system capacity would have to include strongly case-specific infrastructure costs whose estimation is out of the scope of the present paper.

Assumptions 2.1—2.1 allow centering the problem of seeking the most economical pumping infrastructure and operational conditions on finding the most economical pipeline diameter, solids concentration and slurry flow.

2.2. Cost function

The cost function is an extension to that defined in Ihle (2013) with the addition of a cost term associated to the steel/infrastructure cost, $\dot{\Omega} = \theta_W Q_w + \theta_E \dot{E} + \theta_{wgt} \dot{P}_0$, where $\dot{x} \equiv dx/dt$ (time derivatives). Here, the first term stands for the costs of water per unit time, the second corresponds to pumping power and the third corresponds to the (present) cost of pipe steel per unit time. The latter term can be more conveniently expressed as a fixed cost, spent at the beginning of the project, $P_0 = Pt/\tau$, where P is the weight of (constant diameter) pipe material required in the facility, and τ is the operational time frame of the project (Peters et al., 2002, discusses, for the case of transport of homogeneous fluids, a more general investment scenario which, for the sake of obtaining an explicit expression for the economic diameter is not pursued herein). Here, Q_w is the volume flow of water (expressed as $\frac{\text{volume}}{\text{time}}$) and $\dot{E}$ is the flow of energy (expressed as $\frac{\text{energy}}{\text{time}}$). Unit costs are expressed as $\frac{\text{currency}}{\text{unit volume of water}}$ for θ_W and $\frac{\text{currency}}{\text{unit energy}}$ in the case of θ_E. The pipeline steel unit cost, θ_{wgt} is expressed as $\frac{\text{currency}}{\text{unit weight of steel}}$ and represents all possible fixed costs, including amortization, maintenance costs and construction (see Durand et al., 2010, for a detail). A discussion of potential values for the first two terms in a mining context are discussed in Ihle and Kracht (2018). The latter expression for $\dot{\Omega}$ can be therefore expressed in a more simple form as:

$$\dot{\Omega} = \theta_W Q_w + \theta_E \max\{\dot{E}, 0\} + \theta_{wgt}\frac{P}{\tau}. \tag{1}$$

The positive enforcing of the second term of right hand side of energy term is justified by the limitation corresponding to assumption 2.1 above. The reason to express (1) in units of flow of currency (currency over time), rather than simply currency, is that it allows to cast its components in units more familiar to hydraulic transport of solids.

From a mass balance standpoint, the terms related to energy and water use can be related to the solid throughput (*e.g.* concentrate throughput), G (normally imposed as a plant production goal) as:

$$G = Q_{sl}\rho_s\varphi, \tag{2}$$

where Q_{sl} is the slurry flow and φ is the volume fraction of solids. The water flow can be obtained from the latter as $Q_w = Q(1-\varphi)$, and therefore, in terms of the throughput and the solids concentration,

$$Q_w = \frac{G}{\rho_s}\left(\frac{1}{\varphi} - 1\right). \tag{3}$$

The cost of energy can be expressed by means of an energy balance between two arbitrary points in the pipeline. To account for the energy consumption throughout the whole length of the system, it is convenient to consider both the start (pump station), whose tube length position and altitude are $(x, z) = (0, z_{PS})$ ($z_{PS} = z(x=0)$), and the delivery point, at $(x, z) = (L, z_L)$, with $z_L = z(x = L)$. After an energy balance, the corresponding required pumping power is:

$$\dot{E} = \left[\Delta z + \frac{8}{\pi^2}\left(\frac{fL}{D} + k\right)\frac{Q_{sl}^2}{gD^4}\right]\frac{\rho_{sl} g Q_{sl}}{\eta}, \tag{4}$$

with $\Delta z = H + z_L - z_{PS}$. The parameter $H > 0$ is any other constant point energy dissipation, *e.g.*, required for ensuring pressures above the vapor value everywhere in the system in cross-country pipelines. As H is positive, the least energy consumption in relation to dissipation is related to the lowest possible value of H (Ihle, 2016), which is, in particular, independent of the system diameter (singular pressure losses are typically imposed using a number of chokes in the line). On the other hand, f is the Darcy friction factor, k is a minor singular loss coefficient due *e.g.* to valves, elbows, etc. The variable g is the magnitude of the acceleration of gravity, L is the overall length of the pipeline, η is the pump efficiency and ρ_{sl} is the density of the slurry. It is noted that commonly industrial slurry transport systems feature internal diameters above 3 inches, and span distances from several hundred meters to several hundreds of kilometers. From a constructive point of view, smooth paths are promoted to avoid pipe damage due to abrasion, and therefore singularities are scarce or inexistent. An order of magnitude approach to (4) suggests that given $f \sim 10^{-2}$, $k \sim 10^{-1}$, $L \sim e3m$ (up to $e5m$) and $D \sim e-1m$ implies that $fL/D \gg k$ and thus singular losses in this kind of system are negligible, and the energy consumption due to pumping can be expressed as:

$$\dot{E} \approx \left(\Delta z + \frac{8}{\pi^2}\frac{fLQ_{\mathrm{sl}}^2}{gD^5}\right)\frac{\rho_{\mathrm{sl}} g Q_{\mathrm{sl}}}{\eta}. \tag{5}$$

This simplification corresponds to assumption 2.1.

The density of the slurry can be expressed in terms of the solid volume fraction as:

$$\rho_{\mathrm{sl}} = \rho_{\mathrm{s}}\varphi + \rho_{\mathrm{f}}(1-\varphi), \tag{6}$$

with ρ_{s} and ρ_{f} the density of the solids and fluid phase, respectively.

The statement $\max\{\dot{E}, 0\}$ in (1) is the analytical expression of assumption 2.1 and is equivalent to impose that $\Delta z \geq -\frac{8}{\pi^2}\frac{fLQ_{\mathrm{sl}}^2}{gD^5}$. In particular, the sign of Δz is arbitrary, depending on the result of the relation between dissipation and altitude of both the pump station and delivery point. A possible case at this point is when the pump station is high enough to exceed pressure losses by friction at the throughput of interest, requiring no external energy to deliver solids. When this occurs (*i.e.*, the energy term becomes negative) then the excess kinetic energy can be either converted to electrical energy through a generation system or dissipated. If no extra energy consumption is added, then the system would adjust itself to a new equilibrium point corresponding to a higher throughput.

The present approach is based on the observation that industrial steel pipeline vendors often quote pipelines by unit weight of material (Reliable Pipes, 2018; Aesteiron, 2020), and thus differs from the common costing scheme, proportional to D^n, where $n \approx 1.5$ for carbon steel pipe (see Durand et al., 2010, for updated values and materials different than carbon steel). A limitation of this approach is the need to update not just the pipe unit cost but also the exponent n, which is not information that can be obtained straightforward from pipeline vendors and/or contractors. This approach preclude to use direct unit costs from vendors and, as is observed below, becomes impractical when non-economical cost metrics are introduced for decision making.

Considering pipe costs per unit length the n-dependence is obtained by replacing the third term of the right hand side of (1) by

$$\theta_{\mathrm{wgt}}\frac{P}{\tau} := \frac{\theta_{\mathrm{len}} L}{\tau}\left(\frac{D}{D_{\mathrm{ref}}}\right)^n, \tag{7}$$

where θ_{len} accounts for fixed costs, and has units of $\frac{\text{currency}}{\text{pipe length}}$ and D_{ref} is a reference diameter scale (often considered as 1inch, Sarchet and Colburn, 1940).

The corresponding optimization problem to be solved is:

$$\dot{\Omega}^* = \min_{\varphi, D, Q} \dot{\Omega}, \tag{8}$$

subject to the following constraints:

$$U \geq U_{\mathrm{dep}} \tag{9a}$$

$$\varphi \leq \varphi_{\max} \tag{9b}$$

$$p_{\min} < p(x) < p_{\max}, \text{ with } 0 \leq x \leq L \tag{9c}$$

here, U_{dep}, $\varphi_{\max}$, $p_{\min}$ and $p_{\max}$ are the deposit velocity, maximum allowable concentration, minimum and maximum allowable pressure, respectively. An implication of (9a) is that the present method is inadequate for slurries which are transported in laminar flow, such as some high concentration sludges. On the other hand, the pressure constraint (9c) imposes materials and constructive conditions that the pipeline should withstand according to an applicable standard both in front of negative and positive relative pressures.

Considering that available commercial pipeline diameters are available in a discrete fashion, the problem is naturally a discrete one. Although the approach proposed herein is continuous, to adapt it to a discrete one is straightforward by means of approximating results, either to closest commercial values or closest higher ones, depending on the design criteria.

3. Dimensionless cost function

It is convenient to cast the optimization problem (8) into a dimensionless one. To this purpose, a set of (arbitrary) scales is proposed. Then the required flow restrictions, and the pipe thickness modeling are expressed in terms of dimensionless variables to finally solve the new optimization problem.

3.1. Normalization for φ and D

The solid balance statement given by (2) allows to reduce from three to two the independent variables initially posed in (1), namely φ and D.

For dimensional analysis purposes, it is convenient to re-scale variables in terms of the representative parameters in the system. According to Ihle (2016), the most economical water and energy cost is achieved at rather high concentrations, close to the solids deposition limit. This suggests the following definition of normalized concentration:

$$\phi \equiv \frac{\varphi}{\varphi_{\max}}. \quad (0 < \phi \leq 1) \tag{10}$$

In the case of the pipeline diameter, apart from the tube length (L) there is not an external variable that, at first sight, could be on the order of the optimal pipeline diameter. The solid deposit formation process is the result of the interplay between particles and the flow characteristics, including turbulence, when present. It is assumed that a spherical fluid parcel of a single particle of diameter d has a kinetic energy $\mathrm{KE_f} \sim \frac{1}{2} m_{\mathrm{f}} U_{\mathrm{dep}}^2$, where U_{dep} is the corresponding mean flow velocity and $m_{\mathrm{f}} = \frac{\pi d^3}{6}\rho_{\mathrm{f}}$ its mass. On the other hand, the required work to move a single solid particle of the same volume and density ρ_s from the bottom to the top of the tube section can be scaled in terms of its potential energy, $\mathrm{PE}_s = m_s g D$, with $m_s = \frac{\pi d^3}{6}\rho_s$ the particle mass. Assuming that the flow stream should provide sufficient energy to keep particle above the bottom, the order-of-magnitude balance $\mathrm{KE_f} \sim E_s$ is assumed to hold. Solving for U_{dep} results in the following scale for U_{dep}:

$$U_{\mathrm{dep}} \sim \sqrt{2gD(S-1)}, \tag{11}$$

where $S = \rho_{\mathrm{s}}/\rho_{\mathrm{f}}$ is defined as the specific solids gravity. If the mean flow velocity of a particular slurry stream U verifies $U \gg U_{\mathrm{dep}}$ then it is expected that no particles will have the opportunity to settle at the bottom of the pipeline. If, on the other hand, $U \ll U_{\mathrm{dep}}$, solids will form a deposit at the bottom of the pipeline. To account for such critical condition (named to as the *deposit limit*), it is common to define the Durand dimensionless number

$$F_L \equiv \frac{U_{\mathrm{dep}}}{\sqrt{2gD(S-1)}}, \tag{12}$$

so the unknowns U_{dep} and D can be condensed in the independent dimensionless positive parameter F_L. Experimental evidence shows that in general $F_L \sim 1$ (Parzonka et al., 1981; Poloski et al., 2010). The expression (11) has been obtained in the absence of other particles or, in other words, disregarding the role of the particle concentration. This factor might be relevant in industries such as dredging, where particles are on the order of the millimeter. In the mining industry, where comminution products are often below 100 μm in diameter, the effect of φ is slight, as is shown on the (extrapolated) curves in the pioneering work of Durand and Condolios (1952) or the more recent version of Miedema (2016). For moderate to high concentrations ($\varphi \gtrsim 0.25$), experimental evidence suggests that F_L is, again, weakly dependent on the particle concentration for a wide range of particle sizes (Parzonka et al., 1981) and thus can, in first order be treated as a constant value. This argument validates assumption 2.1.

The scale of the deposit velocity can be related both to the particle concentration and the throughput. The mean flow velocity can be expressed in terms of the slurry flow as $U = Q_{\mathrm{sl}}/A$, with $A = \pi D^2/4$ the cross-sectional area of the pipeline. Also, as $U \sim U_{\mathrm{dep}}$ near optimal water and energy consumption, solving for D, the following pipeline diameter scale is proposed:

$$D_* = \left[\frac{2^{3/2}G}{\pi\varphi_{\max}\rho_s g^{1/2}(S-1)^{1/2}}\right]^{2/5}. \tag{13}$$

This relation allows to define a dimensionless pipeline diameter, $\mathscr{D} = D/D_*$ in terms the external properties G, $\varphi_{\max}$, ρ_s and ρ_f. It is noted that so far there are not rigorous bounds for D that have been adopted in the definition of the scale, and therefore, $\mathscr{D} \gtrless 1$ and possibly, but not necessarily, $\mathscr{D} \sim 1$.

Considering the dimensionless variables ϕ and $\mathscr{D}$, dividing the optimization equation (8) by $\rho_s\theta_C$ (θ_C being an arbitrary unit cost scale), the following dimensionless cost function is obtained:

$$\dot{\omega} = K_W\left(\frac{1}{\varphi_{\max}\phi} - 1\right) + \max\left\{K_E\left[1 + \frac{1}{S}\left(\frac{1}{\varphi_{\max}\phi} - 1\right)\right] \times \left[Z + \frac{f(S-1)}{\phi^2\mathscr{D}^5}\right], 0\right\} + K_{P0}\tilde{e}(\mathscr{D} + \tilde{e}), \tag{14}$$

where the dimensionless constants $K_{(\cdot)}$ and Z, along with the newly defined variable $\tilde{e}$, corresponding to the dimensionless pipe wall thickness, are given by:

$$K_W = \frac{\theta_W}{S\rho_f\theta_C} \quad (\geq 0) \tag{15a}$$

$$K_E = \frac{\theta_E gL}{\theta_C\eta} \quad (> 0) \tag{15b}$$

$$Z = \frac{\Delta z}{L} \quad (\gtrless 0) \tag{15c}$$

$$K_{P0} = \frac{\pi\theta_{\mathrm{wgt}}L{D_*}^2\rho_{\mathrm{wall}}}{G\theta_C\tau} \quad (> 0) \tag{15d}$$

$$\tilde{e} = \frac{e}{D_*}. \quad (> 0) \tag{15e}$$

It is noted that, for convenience, (15d) is expressed in terms of the diameter scale D_*, defined in (13).

3.2. Flow restrictions

Flow regime restriction. In Newtonian, and even in a number of non-Newtonian fluids featuring a dual plastic-fluid behavior delimited by a yield stress, the critical laminar-turbulent transition is most commonly defined in terms of a single parameter — the Reynolds number: $Re = \rho_{\mathrm{sl}}UD/\mu$, where μ is the equivalent fluid viscosity (dependent of the particle concentration) at the relevant shear rate. Several models for laminar-turbulent transition condense the transition into one single parameter (Guzel et al., 2009; Eshtiaghi et al., 2012). In these cases, the applicable restriction for minimum laminar-turbulent transition is $Re > Re_{\mathrm{crit}}$, where Re_{crit} is the minimum Reynolds number that ensures turbulent (and not transitional) flow.

At fully developed turbulent flow the friction factor decreases with the Reynolds number. Experimental examples of this trend with Newtonian and non-Newtonian fluids can be found in Draad et al. (1998), whereas a comparison between various models is described in Alderman and Haldenwang (2007) and Ihle et al. (2014). Therefore, in this condition $Re \geq Re_{\mathrm{crit}}$ implies that $f \leq f_{\mathrm{crit}}$ (f is the friction factor corresponding to turbulent flow), where $f_{\mathrm{crit}} = f(Re_{\mathrm{crit}})$. From (14), it follows that:

$$\dot{\omega} \leq K_W\left(\frac{1}{\varphi_{\max}\phi} - 1\right) + \max\left\{K_E\left[1 + \frac{1}{S}\left(\frac{1}{\varphi_{\max}\phi} - 1\right)\right] \times \left[Z + \frac{f_{\mathrm{crit}}(S-1)}{\phi^2\mathscr{D}^5}\right], 0\right\} + K_{P0}\tilde{e}(\mathscr{D} + \tilde{e}), \tag{16}$$

and the equality corresponds to the particular case $f = f_{\mathrm{crit}}$.

Defining bounds of f above f_{crit} is equivalent to impose that the flow is allowed to be transported in laminar flow regime. In particular, $f_{\mathrm{crit}} < f_{\mathrm{lam}}$ for all possible values of f_{lam} where the latter is a friction factor corresponding to the laminar regime (Metzner and Reed, 1955). If, conversely, an upper bound for the cost function is set with $f' < f_{\mathrm{crit}}$ (being f' within the turbulent regime), then $\dot{\omega}(f') > \dot{\omega}(f_{\mathrm{crit}})$. This is shown in Section 3.4, after establishing an explicit form for the last term of the right hand side of expression (16).

Normalized deposit velocity. The length scale for the pipeline diameter is useful to express flow properties as a function of the dimensionless diameter. Noting that $U \geq U_{\mathrm{dep}}$, it is equivalent to write, using (2) and (11), that $\frac{2^{3/2}G}{\varphi\rho_s\pi D^{5/2}g^{1/2}(S-1)^{1/2}} \geq F_L$, which yields the inequality $D \leq D_*\left(\frac{1}{F_L}\frac{\varphi_{\max}}{\varphi}\right)^{2/5}$ or, equivalently,

$$\mathscr{D} \leq \left(\frac{1}{F_L\phi}\right)^{2/5}. \tag{17}$$

In contrast with the definition of $\mathscr{D}$, which can take values greater or lower than the unity, the relation (17) corresponds to a rigorous bound for $\mathscr{D}$, a direct consequence of (9a).

The inequality (17) can be recast in terms of a normalized parameter λ ($0 < \lambda \leq 1$) as:

$$\mathscr{D} = \frac{\lambda}{(F_L\phi)^{2/5}}, \tag{18}$$

thus allowing expressing the dimensionless diameter $\mathscr{D}$ explicitly in terms of the normalized concentration and the Durand number.

3.3. Pipeline thickness modeling

So far, it is not possible to treat the cost function (14) as a continuous function because no explicit form of the dimensionless

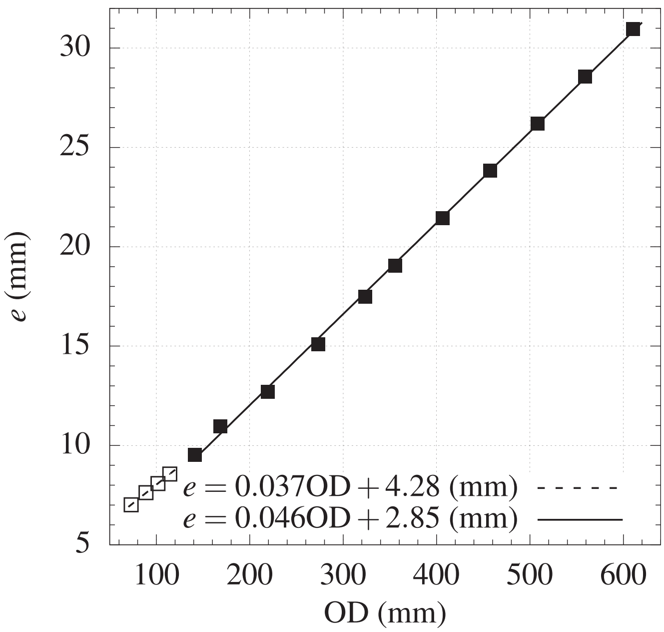

Fig. 1. Example of a typical linear dependence of the pipe thickness with the outside diameter ($\mathrm{OD} = D + 2e$). Here, OD and thickness values correspond to SCH 80 pipelines following Christensen et al. (2004).

wall thickness $\tilde{e}$ has been given. The pipeline thickness, e, depends on the specific standard that rules the pipeline. In the case of high pressure tubes, it is common to follow industrial standards defining steel pipeline thicknesses in terms of their outside diameter ($\mathrm{OD} = D + 2e$). A common example is ASME Standard B36.10M-2004, which groups pipelines according to a *schedule* (SCH) parameter (Christensen et al., 2004). Long distance pipelines for this service often are specified to use thicknesses corresponding to schedule 80, associated to the *strong* specification, where allowable pressures ultimately depend on piping material, outside diameter and working temperature.

A common feature of this infrastructure is that pipe thicknesses are increasing functions of the OD. Fig. 1 shows an example of two linear adjustments that can be made according to the diameter range.

The pipe thickness can be expressed in a linear fashion as:

$$e = \alpha + \beta \mathrm{OD}, \tag{19}$$

where α has dimensions of length and β is dimensionless. This allows to express the las term of the right hand side of (14) as:

$$\tilde{e}(\mathscr{D} + \tilde{e}) = \frac{c_0}{D_*^2} + \frac{c_1}{D_*}\mathscr{D} + c_2\mathscr{D}^2, \tag{20}$$

with:

$$c_0 = \frac{\alpha^2}{(1-2\beta)^2} \tag{21a}$$

$$c_1 = \frac{\alpha}{(1-2\beta)^2} \tag{21b}$$

$$c_2 = \frac{(1-\beta)\beta}{(1-2\beta)^2}. \tag{21c}$$

The dominant term among the three of them will depend on the diameter range. In particular, for very large diameters the third term of the right hand side of (20) dominates over the second, whereas the opposite is expected for very small diameter facilities. In the example of Fig. 1, c_0, proportional to α^2, is negligible in front of the other two terms for all the diameters revised ($\mathrm{OD} > 60mm$). For $\mathrm{OD} = 100mm$ the second and third terms are of the same order of magnitude, whereas increasing the pipeline diameter towards 500 mm makes the third term about 5 times larger than the second. A similar tendency is observed with higher diameters, lower pressure rating pipelines following the same standard.

Considering this approach, the simpler case of a prescribed, constant thickness e_0, independent of OD, as in some custom made pipelines in large scale projects, corresponds to the parameter setting $c_0 = e_0^2$, $c_1 = e_0$ and $c_3 = 0$. In compact form, the dimensionless pipeline cost component corresponding to the third term of the right hand side of (14), can be expressed in terms of λ and F_L as:

$$\frac{\theta_{\mathrm{wgt}} P}{G\theta_{\mathrm{C}}} = K_{\mathrm{P}a}\frac{\lambda^a}{(F_L\phi)^{2a/5}}, \quad (a = 1 \text{ or } 2) \tag{22}$$

where $a = 1$ is the case of prescribed pipe wall thickness (OD-independent) or very small pipeline diameters and $a = 2$ (OD-dependent pipe wall thickness) applies for large diameters. The dimensionless constant K_{Pa} is given accordingly by:

$$\frac{K_{\mathrm{Pa}}}{K_{\mathrm{P0}}} = \begin{cases} \dfrac{e_0}{D_*} & \text{if} \quad a = 1 \quad (\mathrm{OD} - \text{independent pipe wall thickness}) \\ c_2 & \text{if} \quad a = 2, \end{cases} \tag{23}$$

where e_0 is the value of the constant pipe wall thickness and K_{P0} is given by (15d). In the less interesting case of small pipeline diameter, where also $a = 1$, $K_{\mathrm{P}a}/K_{\mathrm{P0}} = c_1/D_*$, where c_1 is given by (21b). Here, the coefficient c_0 has been neglected under the hypothesis that the pipeline wall thickness is significantly smaller than its diameter (and, even more, the square of the thickness in comparison with the square of the diameter).

When the Genereaux-type of cost scheme is used, then (22) is still valid provided

$$K_{\mathrm{P}a} = \frac{\theta_{\mathrm{len}} L}{\tau G\theta_{\mathrm{C}}}\left(\frac{D_*}{D_{\mathrm{ref}}}\right)^n, \tag{24}$$

and $a = n$.

3.4. Normalized λ-ϕ cost function

Replacing (18) and (23) into (14) allows to express the cost function in terms of F_L and the normalized variables λ and ϕ:

$$\dot{\omega} = K_{\mathrm{W}}\left(\frac{1}{\varphi_{\max}\phi} - 1\right) + \max\left\{K_{\mathrm{E}}\left[1 + \frac{1}{S}\left(\frac{1}{\varphi_{\max}\phi} - 1\right)\right] \times \left[Z + \frac{f(S-1)F_L^2}{\lambda^5}\right], 0\right\} + K_{\mathrm{P}a}\frac{\lambda^a}{(F_L\phi)^{2a/5}}, \tag{25}$$

with K_{Pa} given by (23).

The relation (16) expresses an upper boundary for the cost function given that $f \le f_{\mathrm{crit}}$ ($\dot{\omega} \ge \dot{\omega}_{\mathrm{crit}}$, with $\dot{\omega}_{\mathrm{crit}} \equiv \dot{\omega}(f = f_{\mathrm{crit}})$). If, on the other hand, $f < f_{\mathrm{crit}}$ (within the turbulent flow) the solution of the problem (8) is sub-optimal in the f-dimension. This can be seen expressing the friction factor in the generic form $f \sim b_1 Re^{-b_2}$, with

b_1 and b_2 positive parameters (*i.e.*, $\mathrm{d}f/\mathrm{d}Re<0$), applicable to the smooth wall turbulence regime. In the case of Newtonian fluids, an empirical fit has been firstly proposed by Blasius as $(b_1,b_2)=(0.316,0.25)$ (Hager, 2003) and has been extended to yield stress fluids by Chilton and Stainsby (1998). The Reynolds number can be expressed in terms of the present set of independent variables as:

$$Re=(\phi F_L)^{2/5}\left[1+\frac{1}{S}\left(\frac{1}{\varphi_{\max}\phi}-1\right)\right]\frac{\mu_0}{\mu}\frac{Re_0}{\lambda}, \tag{26}$$

with $Re_0=\frac{4G}{\pi\mu_0 D_*}$ (μ_0 is the fluid phase viscosity). The friction factor f represents the part of the kinetic energy dissipated by friction. In turbulent flow $f\lesssim 10^{-2}$, and the term Re^{-b_2} acts an order unity correction factor to $b_1\sim f$, which implies that, for Reynolds numbers just above the laminar-turbulent transition number range (~ 4000), $b_1<1$ (*e.g.* Chilton and Stainsby, 1998; Darby, 2001), being $b_1=1$ the value of the exponent for laminar flows. Thus, the term bearing the friction factor is proportional to λ^{b_2-5} ($b_2-5<0$), whereas the pipe material term is proportional to λ^{a-b_2} ($a-b_2>0$). Therefore, as $\lambda\to 0$ (and consequently $Re(\lambda\to 0)\to\infty$), it is seen that the term bearing the friction factor diverges and that of pipe steel vanishes. Thus, for any arbitrary value of $f\le f_{\mathrm{crit}}$ it is possible to find a sufficiently small value of λ such as (i) $Re\ge Re_{\mathrm{crit}}$ (turbulent flow, as required) and (ii) $\dot{\omega}(f)\ge\dot{\omega}(f_{\mathrm{crit}})$. This contradicts (16) except for the case $f=f_{\mathrm{crit}}$ and therefore implies that the value of f that minimizes $\dot{\omega}$ is necessarily f_{crit}. The cost function $\dot{\omega}_{\mathrm{crit}}$, depends on the dimensionless variables λ and ϕ, and therefore solving the original optimization problem (8) is equivalent to solving the problem:

$$\dot{\omega}^*_{\mathrm{crit}}=\min_{\lambda,\phi}\dot{\omega}_{\mathrm{crit}} \tag{27a}$$

$$0<\lambda\le 1 \tag{27b}$$

$$0<\phi\le 1, \tag{27c}$$

where all the referred dimensionless parameters are independent from each other and, with the possible exception of Z, are positive. An advantage of this approach to the problem is that it is based on the notion of critical condition for laminar-turbulent regime (the critical friction factor, f_{crit}) and it is not explicitly dependent on the particular expression of the Reynolds number dependence. Although in the derivation of this result a power law, which is an explicit form of the friction factor, has been used to illustrate the relevance of f_{crit}, a similar reasoning can be applied using implicit derivation based on the hydraulically smooth turbulent flows described by the logarithmic velocity profile. This is the case of the Dodge-Metzner (Dodge and Metzner, 1959) and Wilson-Thomas model (Wilson and Thomas, 1985; Thomas and Wilson, 1987) where, however, their results can be clearly interpreted in a power law fashion as the straight lines in their reported log-log curves show.

4. Results and discussion

4.1. Model

It is straightforward to see from (25), that $\partial\dot{\omega}_{\mathrm{crit}}/\partial\phi<0$ (and also $\dot{\omega}_{\mathrm{crit}}\to\infty$ as $\phi\to 0$), which leads to the conclusion that lowest costs are always related to highest possible transport concentrations (*i.e.* $\phi=1$), where *possible* stands for operational limitations. Concentrations near the maximum packing fraction are commonly related to the risk of pipeline plugging with subsequent rupture after shutdown (Ihle, 2014b). This observation holds in the particular case of negligible pipe material cost ($K_{\mathrm{P}\ \ a}=0$), thus confirming the conclusion in Ihle (2016), obtained with particular rheological parameters and friction factor structure.

The function (25) has an explicit dependency on the Durand number, F_L. Differently from the already referred weak dependence of F_L with the particle concentration that constitutes assumption 2.1, and also the weak dependence of this variable with the pipeline diameter (Miedema and Ramsdell, 2015), there is a stronger correlation with particle size. Such relationship is not monotonic (Miedema and Ramsdell, 2015, pointed out from their experimental compilation that highest values of F_L, close to 1.6, were found for values of φ between 0.15 and 0.2). On the low-end of F_L values are those related to small particle sizes, where Durand numbers can be between 0.2 and 0.8 depending on their size and density (Parzonka et al., 1981). In relation to (25), increasing the values for the Durand number cause an increase of the relevance of the friction loss term and, on the contrary, causes a decrease of the pipe weight term. This is reasonable, as from (12), higher values of F_L are related to higher minimum velocities which, as the energy consumption is on the order of $U^2 Q_{\mathrm{sl}}\propto U^3$, impose larger amounts of energy to keep particles suspended. Given a fixed throughput, this is related, by virtue of (2), to comparatively lower pipeline sections, thus making relatively less important the third term of the cost expression.

Assuming that $Z+\frac{f_{\mathrm{crit}}(S-1)F_L^2}{\lambda^5}>0$ for all possible values of λ, the rate of change of $\dot{\omega}_{\mathrm{crit}}$ with λ is expressed as:

$$\frac{\partial\dot{\omega}_{\mathrm{crit}}}{\partial\lambda}=-5K_{\mathrm{E}}\left[1+\frac{1}{S}\left(\frac{1}{\varphi_{\max}\phi}-1\right)\right]\frac{f_{\mathrm{crit}}(S-1)F_L^2}{\lambda^6}+\frac{aK_{\mathrm{P}\ \ a}\lambda^{a-1}}{(F_L\phi)^{2a/5}}. \tag{28}$$

This expression can be either positive or negative depending on the relative weight of terms. On the other hand, the relation (28) is independent of the water unit costs, which is explained by the fact that the water cost term is related to the mass balance in the system and thus is independent of the particular transport conditions. Additionally, it is noted that the dimensionless parameter Z is also absent from (28), which implies, in particular, that the presence of a dissipation station tilting the energy line by a fluid column H to ensure that line pressure is above the vapor value neither affect the optimal diameter nor the optimal concentration.

The expression (28) shows that the cost is positive and diverges when $\lambda\to 0$, which means that it exists λ_-, $0<\lambda_-\le 1$ such as $\partial\dot{\omega}_{\mathrm{crit}}/\partial\lambda<0$. Additionally, as the first and second term of the right hand side have opposite signs, then it is possible, depending on the values of the parameters, that $\partial\dot{\omega}_{\mathrm{crit}}/\partial\lambda=0$ for some value of λ. Solving the equation $\partial\dot{\omega}_{\mathrm{crit}}/\partial\lambda=0$ and $\phi=1$ for λ yields:

$$\lambda_0=\left\{5K_{\mathrm{E}}\left[1+\frac{1}{S}\left(\frac{1}{\varphi_{\max}}-1\right)\right]\frac{f_{\mathrm{crit}}(S-1)}{aK_{\mathrm{Pa}}}\right\}^{\frac{1}{5+a}}F_L^{2/5}. \tag{29}$$

there is, however, no guarantee *a priori* that $\lambda_0\le 1$. Therefore, if $\lambda_0>1$, then $\partial\dot{\omega}_{\mathrm{crit}}/\partial\lambda<0$ and the value of λ that minimizes $\dot{\omega}_{\mathrm{crit}}$ is $\lambda=1$. This reasoning can be condensed in the statement:

$$\lambda_{\mathrm{opt}}=\min\{\lambda_0,1\}. \tag{30}$$

To find out whether λ_0 is lower than the unity the following condition results from (29):

$$\Lambda<1, \tag{31}$$

with

$$\Lambda=5K_{\mathrm{E}}\left[1+\frac{1}{S}\left(\frac{1}{\varphi_{\max}}-1\right)\right]\frac{f_{\mathrm{crit}}(S-1)F_L^{\frac{2(5+a)}{5}}}{aK_{\mathrm{Pa}}}. \tag{32}$$

The two solution possibilities suggested in (30) have two distinct interpretations. When $\lambda_{opt} = \lambda_0 < 1$, the term $F_L^{2/5}$ cancels out in the right hand side of (18), and thus the dimensionless optimal diameter is

$$\mathscr{D}_{opt} = \left\{ 5K_E \left[1 + \frac{1}{S}\left(\frac{1}{\varphi_{max}} - 1\right)\right] \frac{f_{crit}(S-1)}{aK_{Pa}} \right\}^{\frac{1}{5+a}}, \quad (33)$$

which is independent of the deposit limit condition and it is therefore solely controlled by costs (energy and infrastructure), the slurry properties and the critical condition to ensure turbulent flow.

The second possibility is when $\lambda_{opt} = 1$. In this case, again using (18),

$$\mathscr{D}_{opt} = F_L^{-2/5}, \quad (34)$$

where it is noted that this solution is independent of the energy and pipeline costs, as well as on the critical friction factor and fully relies on the depositional mechanism.

$$D_{opt} = \begin{cases} \frac{1}{\pi^{2/5}} \times \left(\frac{40}{n}\right)^{\frac{1}{5+n}} \left(\frac{G}{\varphi_{max}}\right)^{\frac{3}{5+n}} \left\{\frac{\theta_E f_{crit} D_{ref}^n [1+\varphi_{max}(S-1)]\tau}{S\theta_{len}\eta\rho_s^2}\right\}^{\frac{1}{5+n}} & \text{if } \Lambda_3 < 1 \\ \left\{\frac{2^{3/2}G}{\pi\rho_s\varphi_{max}[g(S-1)]^{1/2}F_L}\right\}^{2/5} & \text{if } \Lambda_3 \geq 1, \end{cases} \quad (40)$$

4.2. Dimensional results

The previous results, in consistent units as detailed in page List of symbols, can be summarized in the dimensional expressions that follow.

Optimum volume flow. As previously referred, the optimum volume flow is that which verifies $\varphi = \varphi_{max}$. Thus, using (2),

$$Q_{sl,opt} = \frac{G}{\rho_s\varphi_{max}}. \quad (35)$$

Prescribed pipe wall thickness independent of outside diameter ($a = 1$)

$$D_{opt} = \begin{cases} \left(\frac{40}{\pi^3}\right)^{1/6} \sqrt{\frac{G}{\varphi_{max}}} \left\{\frac{\theta_E f_{crit}[1+\varphi_{max}(S-1)]\tau}{S\theta_{wgt}e_0\eta\rho_{wall}\rho_s^2}\right\}^{1/6} & \text{if } \Lambda_1 < 1 \\ \left\{\frac{2^{3/2}G}{\pi\rho_s\varphi_{max}[g(S-1)]^{1/2}F_L}\right\}^{2/5} & \text{if } \Lambda_1 \geq 1, \end{cases} \quad (36)$$

with

$$\Lambda_1 = \frac{5}{(2\pi)^{3/5}}\left(\frac{G}{\varphi_{max}}\right)^{3/5} \frac{\theta_E f_{crit} F_L^{12/5}[1+\varphi_{max}(S-1)]\rho_s^{2/5}[g(S-1)]^{6/5}\tau}{S\theta_{wgt}e_0\eta\rho_{wall}}. \quad (37)$$

Linear increase of wall thickness with outside diameter ($a = 2$)

Considering the linear fit (19) in terms the parameter β and the dimensionless coefficient $c_2(\beta)$, given by (21c) yields:

$$D_{opt} = \begin{cases} \left(\frac{20}{\pi^3}\right)^{1/7} \left(\frac{G}{\varphi_{max}}\right)^{3/7} \left\{\frac{\theta_E f_{crit}[1+\varphi_{max}(S-1)]\tau}{Sc_2\theta_{wgt}\eta\rho_{wall}\rho_s^2}\right\}^{1/7} & \text{if } \Lambda_2 < 1 \\ \left\{\frac{2^{3/2}G}{\pi\rho_s\varphi_{max}[g(S-1)]^{1/2}F_L}\right\}^{2/5} & \text{if } \Lambda_2 \geq 1, \end{cases} \quad (38)$$

with

$$\Lambda_2 = \frac{5}{4\times(2\pi)^{1/5}}\left(\frac{G}{\varphi_{max}}\right)^{1/5} \frac{\theta_E f_{crit} F_L^{14/5}\rho_s^{4/5}[1+\varphi_{max}(S-1)][g(S-1)]^{7/5}\tau}{Sc_2\theta_{wgt}\eta\rho_{wall}} \quad (39)$$

Genereaux-type pipe cost scheme.

with

$$\Lambda_3 = \frac{5}{n}\times\left(\frac{\pi^2}{8}\right)^{n/5}\left(\frac{G}{\varphi_{max}}\right)^{1-\frac{2n}{5}} \frac{\theta_E f_{crit} F_L^{2\left(1+\frac{n}{5}\right)}[1+\varphi_{max}(S-1)][g(S-1)]^{1+\frac{n}{5}}\rho_s^{2n/5}D_{ref}^n\tau}{S\theta_{len}\eta} \quad (41)$$

4.3. Relative effect of terms

Pipeline length and topography. The present approximation to the solution of the optimal pipeline diameter problem is independent of the pipeline length. Results are, on the other hand, independent of possible high points, station locations and the presence of point dissipation in the system, thus obtaining the same result as in sole water and energy optimization (Ihle, 2016). The independence of L comes from the fact that both the energy consumption and the steel requirement for the pipelines are proportional to their length. A potential exception to consider at this point is that long distance pipelines in hilly topographies commonly operate at high pressures and, under certain circumstances, more than one pump station would be required to split the energy line on more than one segment due to standard industrial material limitations. Examples are the case of Alumbrera and Antamina pipelines, with about 300 km of extension and three pump stations (Derammelaere and Shou, 2002), and Samarco (Brazil) with a tubelength of 398 km and two pump stations (Santos et al., 2009). However, often systems shorter than 200 km use a single pump station and standard high resistance carbon steel.

Sensitivity to throughput and φ_{max}. Eqs. (36) and (38) expose that the strongest dependency of the optimal diameter is of the system throughput, where exponents $1/2$, $3/7$ and $1-2n/5$ are found in the cost- and flow regime-dependent ranges ($\Lambda<1$). This dependency becomes slightly weaker when $\Lambda\geq 1$, where the Durand number appears in the expression for the optimal diameter, opposing its effect to that of the throughput. Comparing the three pipe costing schemes, it is noted that the least sensitive dependency to G corresponds to $a=2$, with an exponent $3/7\approx 0.43$. This value is close to the exponent 0.45 derived by Genić et al. (2012) for water and hydraulically smooth flow in carbon steel pipes, based on the Genereaux equation. The highest sensitivity to the throughput corresponds to the case $a=1$ with an exponent $1/2$.

The optimal diameter is sensitive to the maximum operational concentration ($\varphi_{\rm max}$) in a similar fashion than the throughput. The value of $\varphi_{\rm max}$ affects two terms in (36) and (38): firstly, it multiplies $S-1$ and, on the other hand, it divides G. In the first case, the term $[1+\varphi_{\rm max}(S-1)]^{1/7}$ is order unity for a wide range of values of S (typically between about 2.7 and 5), and values of $\varphi_{\rm max}$ between about 0.2 and 0.4, a range that plausibly covers the full spectrum of turbulent transport possibilities. However, in the second case, with $D_{\rm opt}\propto\varphi_{\rm max}^{-k}$, with $k=1/2$ or $3/7$ the effect of such variations of $\varphi_{\rm max}$ can impact the optimal result between about 41% and 52% for the referred range. Trends are similar in the cases $a=1$ and the Genereaux pipe cost approach.

$$D_{\rm opt,hf}=\begin{cases}\left(\dfrac{40}{\pi^3}\right)^{1/6}\left\{\dfrac{\theta_{\rm E}f_{\rm crit}\tau}{\theta_{\rm wgt}e_0\eta\rho_{\rm wall}\rho_{\rm f}^2}\right\}^{1/6}G^{1/2} & \text{if } a=1\\[2ex] \left(\dfrac{20}{\pi^3}\right)^{1/7}\left\{\dfrac{\theta_{\rm E}f_{\rm crit}\tau}{\theta_{\rm wgt}\eta\rho_{\rm wall}\rho_{\rm f}^2}\right\}^{1/7}G^{3/7} & \text{if } a=2\\[2ex] \dfrac{1}{\pi^{2/5}}\times\left(\dfrac{40}{n}\right)^{\frac{1}{5+n}}\left\{\dfrac{\theta_{\rm E}f_{\rm crit}D_{\rm ref}^n\tau}{\theta_{\rm len}\eta\rho_{\rm f}^2}\right\}^{\frac{1}{5+n}}G^{\frac{3}{5+n}}, & \text{(Genereaux – type pipe cost)}\end{cases}\qquad(42)$$

Sensitivity to the depositional limit. In (36) and (38), F_L has an opposing effect compared to G. In particular, higher values of F_L (towards the unity) tend to push the optimal diameter to lower values. This is interpreted as the requirement to increase the mean velocity to preclude the formation of deposits in the pipeline section.

The pipeline depositional limit is bounded to small values in fine slurries. Poloski et al. (2010) compile a list of F_L values for fine slurries (in their work, they use Froude number notation, Fr, where $F_L=Fr/\sqrt{2}$). The equivalent values for F_L reported are between 0.21 and 0.78 for characteristic particle sizes (d) between $6\mu m$ and $70\mu m$. They propose an empirical model specific for fine particles where, besides confirming that, for engineering purposes the effect of concentration is slight, $F_L\propto d^{0.45}$. It is then expected that, in light of (36) and (38), F_L would be approximately proportional to $d^{-0.18}$. Therefore, the proposed model is weakly sensitive to the particle size.

Effect of the total operation time τ. Larger values of τ are related to capital costs diluted on larger times. This is seen from the dimensional formulation of the optimization problem (1), where relatively higher values of τ might render less important the infrastructure term compared to the energy and water components. As a result, larger total operation times would set optimal values tailored towards lesser energy consumptions, which are related to higher pipeline diameters.

Relative effect of other parameters. The impact of $f_{\rm crit}$ is modest, as seen from the exponent $1/6$ or $1/7$ in (36) and (38) and due to the fact that this parameter does not change significantly under the conditions considered and is, in all cases, on the order of 0.03, as has been extensively documented for a variety of fluids and slurry flows (Alderman and Haldenwang, 2007; Guzel et al., 2009).

The particular case of energy and pipeline steel costs deserves a separate mention and is analyzed in Section 4.6. Other parameters such as the pipe thickness in (36), the pump efficiency and the slurry solids density remain constant for a particular system.

4.4. The particular case of a homogeneous fluid

In the case of an homogeneous fluid there is no restriction on the mean flow velocity, and thus $U_{\rm dep}$ must vanish. This is achieved noting that for any finite value of $F_L\sim\varepsilon$ (arbitrarily small) it is possible to set $\rho_{\rm s}:=\rho_{\rm f}$ and $\varphi_{\rm max}=1$ in (6) (*i.e.*, a single phase). From (18), $\lambda\sim\varepsilon^{2/5}\mathscr{D}$ in the optimal case $\phi=1$. For any value of $\mathscr{D}$ it is possible to set ε_0 such that for $\varepsilon<\varepsilon_0$, $\lambda<1$ and thus the expressions (36), (38) and (40), reflecting independence of the deposit limit, can be used. The corresponding dimensional expressions of the optimum diameter are:

where the prefactors are dimensionless.

4.5. Allowable pressure and optimal diameter

Actual line pressures depend on the difference between the energy line and the topography, the former depending on the frictional pressure losses and required point dissipation and the latter being strongly site-specific. The constraint (9c) requires a feasible space from the point of view of the relationship between pipe pressure rating (including materials, OD and wall thickness) and actual operational pressure. Pressure compliance then requires, after computing the optimal diameter and pipe wall thickness, to verify whether the particular choice of pipeline size and pressure rating is in accordance with such hypothesis. After an energy balance, the pressure under optimal operational conditions, $p(x)$ as referred to in the inequality (9c), needs to verify

$$p(x)=\rho_{\rm sl\ ,max}g\left[\frac{8f_{\rm crit}(L-x)G^2}{g\pi^2\varphi_{\rm max}^2}+H+z_L-z\right],\qquad(43)$$

with $\rho_{\rm sl\ ,max}=\rho_{\rm sl}(\varphi_{\rm max})$ in (6) and $z=z(x)$. Once the pressure rating of the pipeline is set, verifying (9c) and (43) can be ensured setting H or splitting the energy line into several segments adding intermediate pump stations to limit the maximum line pressure (Santos et al., 2009; Ihle and Kracht, 2018). The process of integrating optimal pipe diameters with actual topography and service conditions can be, in this sense, an iterative one. However, using high pressure rating pipes allows considerable flexibility in terms of pressure resistance as a function of pipe length in a wide variety of situations.

A second aspect pertaining pressure compliance, beyond the scope of the present analysis, is related to operational flexibility. It might be desirable that pressure may not exceed $p_{\max}$ for a subset of sub-optimal flow conditions. Provided H is set to the minimum possible value to avoid phase change in the slurry, this can happen for throughputs higher than the design value G, $f < f_{\text{crit}}$ and $\varphi < \varphi_{\max}$. To respond this question, it is required, in particular, to set a particular model for the friction factor f, not just the critical value as required for the determination of the optimal diameter.

4.6. Examples

To obtain an order-of-magnitude comparison between the present approach and existing pipeline facilities with known characteristics are presented. It is noted that there is no intention of validation with known existing pipeline diameters due to:

- Design criteria for the pipeline are not available. This should include the consideration of critical Reynolds numbers for the model, effective deposit velocity assumed and life of the project.
- Key geometric considerations such as the installation of an internal liner to protect the pipeline steel from corrosion affects directly the relation between internal and external diameters.
- Reported throughput in the literature might not correspond to the actual design capacity.

Fine slurries reproduced approximately correspond to iron concentrate, copper concentrate and phosphate slurry. To obtain a quantitative reference on the impact of variations on costs, low and high values for both θ_E (50USD/MWh and 150USD/MWh) and θ_{wgt} (5USD/kg_steel and 50USD/kg_steel) are combined according to the matrix presented in Table A.4 in A. Results are detailed in Table 1, and the calculation hypotheses common to all cost scenarios are given in Table A.5 in the same Appendix.

The results presented in Table 1 show that the algorithm corresponding to (30), and (31) applied to (18) to obtain D_{opt} give results which are, in general, of the same order than those finally built. Of the 17 pipelines reported, in only one of them (Las Truchas), a significant difference between the present computation and the reported diameter was found. However, as previously referred, the tendency observed herein is just to suggest that results of the present model are reasonable. Besides the diameter similarity, there is a consistent prediction of diameters closely below those established by corresponding engineering, as confirmed by the four cost scenarios in Table A.4 analyzed herein. In the case of several copper concentrate pipelines featuring internal HDPE liners, some of the present computations of the internal diameter D_{opt} are even closer. It is also noted that diameters which are below and close to those of real facilities are those associated to lower steel costs. These are cases (1,1) and (2,1), with $\theta_{\text{wgt}} = 5USD/kg$, which yield the highest diameters due to values of Λ greater than 1, implying that such optimal diameters are controlled by the deposit condition rather than unit costs and critical Reynolds numbers. Conversely about 1/4 of the cases feature $\Lambda < 1$.

Present results show that there is a tendency in high tonnage iron concentrate pipelines ($G > 100kg/s$) to be weakly dependent on cost conditions and rather to be fully conditioned by the deposit limit. In these large pipelines, turbulence is much more easily achieved than the deposit condition and a therefore the latter appears as a more restrictive condition.

4.7. Including footprint in costs

In copper concentrate and phosphate slurry lines, the behavior is rather dual in the sense of Λ, depending on the cost scenario. The notion of cost has been treated so far in a rather slack way. Although it is straightforward to interpret it in a supply cost sense, it is possible to define a rather extended version, oriented towards including embodied energy. From a dimensional standpoint, θ_{wgt} is expressed as currency over kg pipeline. This can be extended to a slightly more general definition:

$$\theta_{\text{wgt}} = \theta_{\text{wgt}\quad s} + \theta_{EE}EE, \tag{44}$$

where θ_{wgts} represents supply costs and θ_{EE} might be associated to embodied energy and has units of $\frac{\text{currency}}{\text{unit energy}}$. The term corresponds to the embodied energy, and may or may not be relevant depending on aspects such as the supply chain related to the pipeline. For instance, assuming an average cradle to gate value (European origin) of $EE = 9.6e-3MWh/kg$ (Hammond and Jones, 2008), and

Table 1
Calculation examples in terms of the cost scenarios denoted in brackets as (i,j), with i and j either 1 or 2, described in Table A.4 of A, for SCH 80, steel pipeline following the ASME standard detailed in Christensen et al. (2004). The nominal diameter has been approximated as the closest commercial value greater than the computed one. Computational hypotheses are given in Table t:example_calc_hypotheses. Values of Λ have been rounded to the first decimal place.

Ore type	ρ_s	d	F_L	G	OD_{opt} (Λ) for various scenarios				Facility with similar throughput
	(kg/m^3)	(μm)		(kg/s)	(1,1)	(1,2)	(2,1)	(2,2)	
Iron concentrate	4760	44	0.45	64.7	8 in (3.1)	7 in (0.3)	8 in (9.4)	8 in (0.9)	Savage River, Australia, 9 in, 86km[a]
				51.8	8 in (3.0)	6 in (0.3)	8 in (9.0)	7 in (0.9)	Pena, USA, 8 in, 45km[a]
				43.2	7 in (2.9)	6 in (0.3)	7 in (8.7)	7 in (0.9)	Las Truchas, Mexico, 10 in, 27km[a]
				60.4	8 in (3.1)	7 in (0.3)	8 in (9.3)	8 in (0.9)	Sierra Grande, Argentina, 8 in, 32km[a]
				523.21	20 in (4.8)	18 in (0.5)	20 in (14.3)	20 in (1.4)	Samarco line 1, Brazil, 18/20/22 in, 398km[b]
				237.8	14 in (4.1)	12 in (0.4)	14 in (12.2)	14 in (1.2)	Samarco line 2, Brazil, 14/16 in, 398km[b]
				840.3	24 in (5.2)	22 in (0.5)	24 in (15.7)	24 in (1.6)	Minas Rio, Brazil, 24/26 in, 529km[c]
Copper concentrate	4300	44	0.45	28.8	6 in (2.1)	5 in (0.21)	6 in (6.4)	6 in (0.6)	Bougainville, PNG, 6 in, 32km[a]
				8.6	4 in (1.7)	3 in (0.2)	4 in (5.0)	3.5 in (0.5)	West Irian, Indonesia, 4 in, 111km[a]
				11.5	5 in (1.8)	3.5 in (0.2)	5 in (5.3)	4 in (0.5)	Pinto Valley, USA, 4 in, 17km[a]
		60	0.5	28.8	6 in (2.8)	5 in (0.3)	6 in (8.5)	6 in (0.9)	Collahuasi, Chile, 7 in, 203km[a] (lined)
				23.0	6 in (2.7)	5 in (0.3)	6 in (8.2)	6 in (0.8)	Alumbrera, Argentina, 6 in, 314km[a] (lined)
				47.6	8 in (3.1)	6 in (0.3)	8 in (9.4)	7 in (0.9)	Antamina, Peru, 9/12 in, 300km[d] (lined)
				34.9	7 in (3.0)	6 in (0.3)	7 in (8.9)	7 in (0.9)	Los Pelambres, Chile, 8 in, 120km[d] (lined)
	4360			41.1	7 in (3.2)	6 in (0.3)	7 in (9.5)	7 in (1.0)	Minera Escondida, Chile, 6/7 in, 166km[e] (lined)
Phosphate slurry	2850	125	0.7	71.9	10 in (3.3)	9 in (0.3)	10 in (9.9)	10 in (1.0)	Chevron, Vernal, USA, 10 in, 152km[a]
				63.4	9 in (3.2)	8 in (0.3)	9 in (9.7)	9 in (1.0)	Valep, Brazil, 10 in, 120km[f]

References: [a]Abulnaga (2002); [b]Santos et al. (2009); [c]Ausenco (2018); [d]Derammelaere and Shou (2002); [e]Betinol and Jaime (2004); [f]Jacobs (1991).

a reference unit energy cost of $\theta_{EE} = 100 USD/MWh$ yield a correction in $\theta_{\rm wgt}$ of $0.96 USD/kg$. In the Australian context, Lenzen and Dey (2000) report a slightly higher value of $\rm EE = 1.1e-2MWh/kg$. Values for Brazil, China, India, Mexico and South Africa are reviewed on Price et al. (2002) and, more recently in the case of China (reporting $6.4e-3\rm MWh/kg$) and US ($4.1e-3\rm MWh/kg$) in Hasanbeigi et al. (2014). The role of distance and transport has been reviewed by Gleick and Cooley (2009) using North American data of energy costs both in terms of the weight and the distance for cargo ship ($1.03e-4\rm kWh\ ton^{-1}km^{-1}$) and heavy truck transportation ($1.03e-4\rm MWh\ ton^{-1}km^{-1}$). The parameter $\theta_{\rm wgt}$ can thus be adapted as a means of cradle to gate assessment of different supply and transport options. Analysis can be made either considering a one-to-one cost comparison, as shown in (44), or giving weighting factors for $\theta_{\rm wgts}$ and θ_{EE}.

The same concept can be used, in the case of the energy cost component, to include the impact of the energy source on the carbon footprint when there is more than one sourcing option. In general, $\theta_{\rm E}$ and $\theta_{\rm wgt}$ can be understood as weighting factors for decision making, where the final decision include the pipeline diameter as a key factor.

5. Final remarks

Modern pipeline systems need to face a number of strong restrictions that range from the economical and resourcing (water and energy) to environmental. New future pipeline designs need to cope with these new restrictions from the conception phase, where there engineering is continuously challenged to be less and less conservative in their conceptions. The present formulation for the optimal concentration and diameter shows that a multi-million investment may be adjusted quantitatively following modern environmental metrics that are blended together with engineering requisites for proper operation.

The present model has been focused on the formulation of a simple, though physically-based model for the problem of slurry pipeline design in the potential presence of multiple scenarios for commodity supply (steel and energy costs), where the nature of the sources can be relevant and thus would need to be analyzed in the context of engineering design and operation. Added to imposing the condition of turbulent flow, a deposit formation limit has been included, where both restricting conditions have been referred depending of key parameters governing them rather than using particular models explicitly.

One of the outcomes of the present work is the possibility to explicitly isolate the unit cost of pipeline materials. Results have been found to be consistent with previous approaches to this cost estimation. However, a significant conceptual difference with past approaches is the independence of results with market fluctuations, except by unit costs of energy and pipeline material.

The more general problem of economic pipe diameter for strongly stratified slurries has not being tacked herein, featuring a static or sliding bed was not pursued, but appears as a natural extension of the present model.

Acknowledgements

The author gratefully acknowledge support from the Department of Mining Engineering Universidad de Chile and fruitful conversations with Mr Pedro Valencia (SHIMIN Engineering). The author also acknowledges support from The Chilean Agency for Research and Development (ANID) through PIA Grant AFB180004.

List of symbols

a	modeling case parameter (Eq. (22)), OD-independent wall thickness or very small pipe diameter ($a = 1$) or linear function of OD ($a = 2$) (dimensionless)
c_0	model parameter (length^2, Eq. (21a))
c_1	model parameter (length, Eq. (21b))
c_2	model parameter (dimensionless, Eq. (21c))
d	particle characteristic size (length)
D	pipeline diameter (length)
$D_{\rm opt}$	pipeline optimal diameter (length)
$D_{\rm opt,hf}$	homogeneous fluid pipeline optimal diameter (length)
$D_{\rm ref}$	reference (dimensional) diameter (length, Eq. (7))
D_*	pipeline (dimensional) diameter scale (length, Eq. (13))
$\mathscr{D}$	dimensionless pipeline diameter ($= D/D_*$)
$\mathscr{D}_{\rm opt}$	optimal dimensionless pipe diameter
$\dot{E}$	energy consumption (energy/time)
e	pipeline wall thickness (length)
e_0	prescribed pipe wall thickness (length)
$\tilde{e}$	dimensionless pipeline wall thickness (length, Eq. (15e))
F_L	Durand number (dimensionless, Eq. (12))
f	Darcy friction factor (dimensionless)
$f_{\rm crit}$	maximum value of f in turbulent flow regime (dimensionless)
G	solids throughput (solid mass/time)
g	magnitude of gravity acceleration (mass/time^2)
$f_{\rm lam}$	friction factor in laminar flow regime (dimensionless)
H	point energy dissipation head (length)
$\rm KE_f$	scale of kinetic energy of fluid parcel (mass length^2/time^2)
$K_{\rm E}$	dimensionless parameter (Eq. (15b))
$K_{\rm P0}$	dimensionless parameter (Eq. (15d))
$K_{\rm Pa}$	dimensionless parameter (Eq. (23))
$K_{\rm W}$	dimensionless parameter (Eq. (15a))
k	singular energy loss coefficient (dimensionless)
L	pipeline length (length)
m_f	mass of fluid parcel (mass)
n	exponent for pipe cost modeling (Eq. (7), dimensionless)
OD	pipeline outside diameter (length)
$\rm OD_{opt}$	nearest higher standard pipeline outside diameter close to optimal value (length)
p	line pressure (mass length^{-1} time^{-2})
P	pipe material mass (mass)
$\rm PE_s$	scale of potential energy of particle (mass length^2/time^2)
$\dot{P}_0$	pipeline material use (pipe material mass/time)
$Q_{\rm sl}$	slurry volume flow (volume/time)
$Q_{\rm w}$	water consumption (volume/time)
Re	Reynolds number (dimensionless)
$Re_{\rm crit}$	minimum Reynolds number for turbulent flow (dimensionless)
S	solid phase specific gravity ($= \rho_s/\rho_f$, dimensionless)
SCH	pipeline schedule ()
t	time
U	mean flow velocity (length/time)
$U_{\rm dep}$	mean flow velocity corresponding to the solid deposit formation limit (length/time)
Z	dimensionless parameter (Eq. (15c))
z_L	discharge point altitude (length)
$z_{\rm PS}$	pump station altitude (length)

Greek letters

α	modeling parameter (length, Eq. (19))

β	modeling parameter (dimensionless, Eq. (19))
Δz	$H + z_L - z_{PS}$ (length)
ε	arbitrarily small parameter (dimensionless)
φ	solids volume fraction (dimensionless)
φ_{max}	maximum feasible solids volume fraction in operation (dimensionless)
ϕ	normalized volume fraction ($= \varphi/\varphi_{max}$, dimensionless)
θ_C	solid unit cost (arbitrary) scale (currency/solid mass)
θ_E	energy unit cost (currency/energy unit)
θ_{len}	pipe cost per unit length (currency/unit length)
θ_W	water unit cost (currency/water volume unit)
θ_{wgt}	pipe material unit cost (currency/pipe weight)
Λ	dimensionless parameter for optimal diameter control mechanism (Eq. (32))
λ	dimensionless parameter (Eq. (18))
λ_{opt}	optimal value of λ (Eq. (30), dimensionless)
μ	concentration-dependent slurry dynamic viscosity (mass length^{-1} time^{-1})
μ_0	fluid phase dynamic viscosity (mass length^{-1} time^{-1})
η	pump efficiency (dimensionless)
ρ_f	fluid phase density mass length^{-3}
ρ_s	solid phase density mass length^{-3}
ρ_{sl}	slurry density mass length^{-3}
ρ_{wall}	pipe wall density mass length^{-3}
τ	life span of operation (time)
$\dot{\Omega}$	cost flow function (currency/time)
$\dot{\omega}$	dimensionless flow function (currency/time)
$\dot{\omega}_{crit}$	$\dot{\omega}(f = f_{crit})$ (dimensionless)
$\dot{\omega}^*_{crit}$	optimal value of $\dot{\omega}_{crit}$ (dimensionless, system 27)

Appendix A. Calculation Hypotheses for example in Section 4.6

Table A.4 presents energy and steel cost scenarios used in the example of Section 4.6. The remaining required input parameters used in the corresponding computations are given in Table A.5.

Table A.4
Cost scenarios developed in examples.

	case designation			
	(1,1)	(1,2)	(2,1)	(2,2)
θ_E(USD/MWh)	50	50	150	150
θ_{wgt}(USD/kg$_{steel}$)	5	50	5	50

Table A.5
Calculation for results given in Table 1.

Variable	Value	Comments
φ_{max}	0.3	Volumetric concentration corresponding to the order-of-magnitude of transport of fine slurries (*e.g.* several facility descriptions in Sec. 5 of Jacobs, 1991)
τ	20 years	Life span of operation
η	0.7	Pump efficiency, as in Ihle and Kracht (2018)
ρ_{wall}	7850 kg/m^3	Density corresponding to high pressure pipeline steel
a	2	Linear increment of pipeline thickness with outside diameter
c_2	0.11929	From (21c), corresponding to using SCH80 data from Christensen et al. (2004)
f_{crit}	0.032	According to Metzner and Reed (1955) (note that in that work the Fanning friction factor, $f_N = f/4$, is used instead of the Darcy value (f), as considered herein)
F_L	(variable)	Computed Durand number, following data of Figure 1 in Miedema and Ramsdell (2015)
OD_{opt}	(variable)	Nearest higher standard pipeline outside diameter close to optimal value (D_{opt})

References

Abulnaga, B.E., 2002. Slurry Systems Handbook. McGraw-Hill, New York.
Alderman, N.J., Haldenwang, R., 2007. A review of Newtonian and non-Newtonian flow in rectangular open channels. In: The 17th International Conference on the Hydraulic Transport of Solids.
Ausenco, 2018. Minas-rio iron concentrate pipeline - featured project. https://www.ausenco.com/en/anglo-american-minas-rio-iron. Accessed on 02/17/2018.
Baeza, D., Ihle, C.F., Ortiz, J.M., 2017. A comparison between ACO and Dijkstra algorithms for optimal ore concentrate pipeline routing. J. Clean. Prod. 144, 149–160.
Betinol, R.G., Jaime, H.E., 2004. Startup of dual concentrate pipeline for minera escondida limitada, phase IV. In: 16th International Conference on Hydrotransport (Santiago, Chile).
Bird, R.B., Dai, G.C., Yarusso, B., 1983. The rheology and flow of viscoplastic materials. Rev. Chem. Eng. 1 (1), 1–70.
Chilton, R.A., Stainsby, R., 1998. Pressure loss equations for laminar and turbulent non-Newtonian pipe flow. J. Hydraul. Eng. 124 (1929), 522–529.
Christensen, F.M., Cohen, A., Gruber, J.A., Holliday, W.N., Ingels, L.T., Karian, J.H., Kverneland, K.O., Machell Jr., A.R., Pollak, P., Rau, R.N., 2004. Welded and Seamless Wrought Steel Pipe Standard. ASME B36.10M-2004.
Darby, R., 2001. Chemical Engineering Fluid Mechanics. CRC.
Derammelaere, R.H., Shou, G., 2002. Antamina?s copper and zinc concentrate pipeline incorporates advanced technologies. In: Proc. Of Hydrotransport Conference, vol. 15, pp. 5–18.
Dodge, D., Metzner, A., 1959. Turbulent flow of non-Newtonian systems. AIChE J. 5 (2), 189–204.
Draad, A.A., Kuiken, G., Nieuwstadt, F., 1998. Laminar–turbulent transition in pipe flow for Newtonian and non-Newtonian fluids. J. Fluid Mech. 377, 267–312.
Durand, A.A., de Villafranca Casas, M.J., Cornejo, A.S.G., Carranza, D.J., Román, F.J.P., Suárez, R.G.S., Espinoza, J.S., Others, 2010. Updating the rules for pipe sizing. Chem. Eng. 117 (1), 48.
Durand, R., Condolios, E., 1952. Transport hydraulique et decantation des materiaux solides (in French). In: Compte Rendu des Deuxiemes Journees de L'Hydraulique. La Houille Blanche, pp. 29–55.
Eshtiaghi, N., Markis, F., Slatter, P., 2012. The laminar/turbulent transition in a sludge pipeline. Water Sci. Technol. 65 (4), 697–702.
Garcia, E.J., Steffe, J.F., 1986. Optimum economic pipe diameter for pumping herschel-bulkley fluids in laminar flow. J. Food Process. Eng. 8 (2), 117–136.
Genereaux, R., 1937. Fluid-flow design methods. Ind. Eng. Chem. 29 (4), 385–388.
Genić, S.B., Jaćimović, B.M., Genić, V.B., 2012. Economic optimization of pipe diameter for complete turbulence. Energy Build. 45, 335–338.
Genić, S., Jaćimović, B., 2018. A shortcut to determine optimal steam pipe diameter. Chem. Eng. Prog. 114 (8), 22–27.
Gleick, P.H., Cooley, H.S., 2009. Energy implications of bottled water. Environ. Res. Lett. 4 (1), 014009.
Guzel, B., Frigaard, I., Martinez, D., 2009. Predicting laminar?turbulent transition in Poiseuille pipe flow for non-Newtonian fluids. Chem. Eng. Sci. 64, 254–264.
Hager, W., 2003. Blasius: a life in research and education. Exp. Fluid 34 (5), 566–571.
Hammond, G., Jones, C., 2008. Inventory of Carbon & Energy: ICE. Sustainable Energy Research Team, Department of Mechanical Engineering, University of Bath.
Hasanbeigi, A., Price, L., Chunxia, Z., Aden, N., Xiuping, L., Fangqin, S., 2014. Comparison of iron and steel production energy use and energy intensity in China and the us. J. Clean. Prod. 65, 108–119.
Ihle, C.F., 2013. A cost perspective for long distance ore pipeline water and energy utilization. Part I: optimal base values. Int. J. Miner. Process. 122, 1–12.
Ihle, C.F., 2014. The need to extend the study of greenhouse impacts of mining and mineral processing to hydraulic streams: long distance pipelines count. J. Clean. Prod. 84, 597.
Ihle, C.F., 2014b. Should maximum pressures in ore pipelines be computed out of system startups or power outages? Miner. Eng. 55, 57–59.
Ihle, C.F., 2016. The least energy and water cost condition for turbulent, homogeneous pipeline slurry transport. Int. J. Miner. Process. 148, 59–64.
Ihle, C.F., Kracht, W., 2018. The relevance of water recirculation in large scale mineral processing plants with a remote water supply. J. Clean. Prod. 177, 34–51.
Ihle, C.F., Tamburrino, A., 2012. Variables affecting energy efficiency in turbulent ore concentrate pipe transport. Miner. Eng. 38, 62–70.
Ihle, C.F., Tamburrino, A., Montserrat, S., 2013. Putting together water, energy, investment and environmental metrics in long distance slurry pipeline projects: an attainable goal. In: Rio Pipeline Conference & Exposition 2013. Brazilian Institute for Oil, Gas and Biofuels (IBP), Rio de Janeiro, Brazil.
Ihle, C.F., Tamburrino, A., Montserrat, S., 2014. Identifying the relative importance of energy and water costs in hydraulic transport systems through a combined physics-and cost-based indicator. J. Clean. Prod. 84, 589–596.
Jacobs, B.E.A., 1991. Design of Slurry Transport Systems. Elsevier.
Lenzen, M., Dey, C., 2000. Truncation error in embodied energy analyses of basic iron and steel products. Energy 25 (6), 577–585.
Metzner, A.B., Reed, J.C., 1955. Flow of non-Newtonian fluids — correlation of the laminar, transition, and turbulent-flow regions. AIChE J. 1 (4), 434–440.
Miedema, S., 2016. Slurry Transport: Fundamentals, a Historical Overview and the Delft Head Loss & Limit Deposit Velocity Framework. SA Miedema/Delft University of Technology.

Miedema, S.A., Ramsdell, R.C., 2015. The Limit Deposit Velocity model, a new approach. J. Hydrol. Hydromechanics 63 (4), 273–286.
Parzonka, W., Kenchington, J.M., Charles, M.E., 1981. Hydrotransport of solids in horizontal pipes: effects of solids concentration and particle size on the deposit velocity. Can. J. Chem. Eng. 59 (3), 291–296.
Paterson, A.J.C., 2012. Pipeline transport of high density slurries: a historical review of past mistakes, lessons learned and current technologies. Min. Technol. 121 (1), 37–45.
Peters, M., Timmerhaus, K., West, R., 2002. Plant Design and Economics for Chemical Engineers, fifth ed. McGraw-Hill Education.
Poloski, A.P., Etchells, A.W., Chun, J., Adkins, H.E., Casella, A.M., Minette, M.J., Yokuda, S.T., 2010. A pipeline transport correlation for slurries with small but dense particles. Can. J. Chem. Eng. 88 (April), 182–189.
Price, L., Sinton, J., Worrell, E., Phylipsen, D., Xiulian, H., Ji, L., 2002. Energy use and carbon dioxide emissions from steel production in China. Energy 27 (5), 429–446.
Reliable Pipes, 2018. Price list of carbon steel pipes & tubes, seamless pipe, welded pipe — reliable pipes & tubes. http://www.reliablepipestubes.com/blog/price-pricelist-carbon-steel-pipe-seamless-pipe-welded-pipe/. Accessed on 02/17/2018.
Ricks, B.L., 2002. Slurry Pipeline Transportation, vol. 2. Society for Mining Metallurgy, pp. 1422–1445. Ch. 10.
Santos, I., Nébias, R.B., Silva, T., 2009. An overview of Samarco's pipelines and their KPI's. In: Proceedings of the Rio Pipeline Conference (Rio de Janeiro, Brazil).
Sarchet, B.R., Colburn, A.P., 1940. Economic pipe size in the transportation of viscous and nonviscous fluids. Ind. Eng. Chem. 32 (9), 1249–1252.
Thomas, A.D., Wilson, K.C., 1987. New analysis of non-Newtonian turbulent flow and yield-power-law fluids. Can. J. Chem. Eng. 65 (2), 335–338.
Turian, R.M., Yuan, T.F., 1977. Flow of slurries in pipelines. AIChE J. 23 (3), 232–243.
Wilson, K.C., Thomas, A.D., 1985. A new analysis of the turbulent flow of non-Newtonian fluids. Can. J. Chem. Eng. 63 (4), 539–546.
Aesteiron. Carbon steel pipes and tubes - Aesteiron steel pipes. http://aesteironsteelpipes.com/35-carbonsteel-pipes-tubes, 2020. Accessed on 04/16/2020.